Hyperfine Coherence in the Presence of Spontaneous Photon Scattering

R. Ozeri, C. Langer, J. D. Jost, B. DeMarco,* A. Ben-Kish,† B. R. Blakestad, J. Britton, J. Chiaverini, W. M. Itano, D. B. Hume, D. Leibfried, T. Rosenband, P. O. Schmidt, and D. J. Wineland

NIST Boulder, Time and Frequency Division, Boulder Colorado 80305, USA

(Received 10 February 2005; published 14 July 2005)

The coherence of a hyperfine-state superposition of a trapped $^9Be^+$ ion in the presence of off-resonant light is studied experimentally. It is shown that Rayleigh elastic scattering of photons that does not change state populations also does not affect coherence. We observe coherence times that exceed the average scattering time of 19 photons which is determined from measured Stark shifts. This result implies that, with sufficient control over its parameters, laser light can be used to manipulate hyperfine-state superpositions with very little decoherence.

DOI: 10.1103/PhysRevLett.95.030403 PACS numbers: 03.65.Yz, 03.65.Ta, 32.80.−t, 42.50.Ct

Superpositions of hyperfine states of atoms have been the subject of considerable experimental interest. A good example is the role they have played in the development of atomic clocks over the last five decades [1]. More recently, hyperfine coherences of quantum-degenerate gases have been used to reveal their intrinsic properties [2,3]. Atomic hyperfine-state superpositions are also being investigated as possible information carriers for quantum information processing [4].

In many such experiments, laser light is used to coherently manipulate the hyperfine superpositions with stimulated Raman transitions. In addition, laser light can be used to trap atoms as in the case of optical-dipole traps. Since light perturbs the energies of hyperfine levels, imperfect control of laser-beam parameters can lead to dephasing of the superpositions and loss of coherence [5–7].

Previous experiments with neutral atoms in dipole traps investigated the coherence of hyperfine superpositions in the presence of light [6,7]. In these experiments the dominant source of dephasing was noise in experimental parameters such as fluctuations in the laser intensity or the ambient magnetic field.

A more fundamental source of decoherence arises from spontaneous scattering of photons [8]. Spontaneous scattering is typically suppressed by detuning the laser frequency from allowed optical transitions, but it cannot be eliminated completely. Generally, if a spontaneously scattered photon carries information about which hyperfine state scattered the light, the event effectively measures the atomic state and the superposition collapses. In contrast, if the scattered photon does not contain this information then coherence is preserved. In this Letter, we verify this effect by means of an experimental study of the hyperfine decoherence of a trapped $^9Be^+$ ion caused by spontaneous scattering of photons from a nonresonant laser beam. Our results show that coherence can be preserved in the presence of spontaneous photon scattering.

Zeeman ground-state coherence was previously studied in the presence of resonant spontaneous photon scattering [9]. Coherence was shown to be preserved when the Zeeman splitting between the two ground states is small with respect to the excited-state natural width.

Off-resonant spontaneous scattering is a two-photon process in which the atom scatters a laser photon into an electromagnetic vacuum mode. Following such a scattering event the atom can be found in the same or a different internal state, corresponding to elastic Rayleigh or inelastic Raman scattering, respectively. The polarization and frequency of a Raman scattered photon depend on the angular momentum and energy imparted to the atom and are therefore entangled with the atomic internal state, as demonstrated in [10]. A single Raman scattering event will therefore completely decohere a hyperfine superposition [11]. In Rayleigh elastic scattering the atom's internal states are not entangled with the scattered photon [12,13]. Therefore, an atom initially prepared in a hyperfine-state superposition will remain in this superposition after the photon was scattered.

The scattering amplitude can be calculated by evaluating the electric-dipole coupling between the initial ground state and the relevant excited state, and between the excited state and final ground state. When there are several excited states, the scattering amplitude is given by a coherent sum over all amplitudes of scattering through the different excited states.

The relevant energy levels in $^9Be^+$ are illustrated in Fig. 1. Light is detuned from the $2s\ ^2S_{1/2} \rightarrow 2p^2P_{1/2,3/2}$ transitions near 313 nm. The $2p\ ^2P_J$ manifold has a fine structure that consists of the $J = 1/2$ and $J = 3/2$ levels, separated by $\Delta_f/2\pi = 197.2$ GHz. The ion is illuminated with a laser beam of intensity I. The laser beam polarization, $\hat{\sigma}_k$, is characterized with respect to the magnetic field, which sets the quantization axis for the ion, where $k = 0$, $+$ or $-$ correspond to parallel to the magnetic field ($\hat{\pi}$) or right or left circular polarization, respectively. The rate of photon scattering events in which an ion initially in state $|i\rangle$ ends up in state $|f\rangle$ is given by the Kramers-Heisenberg formula [14,15],

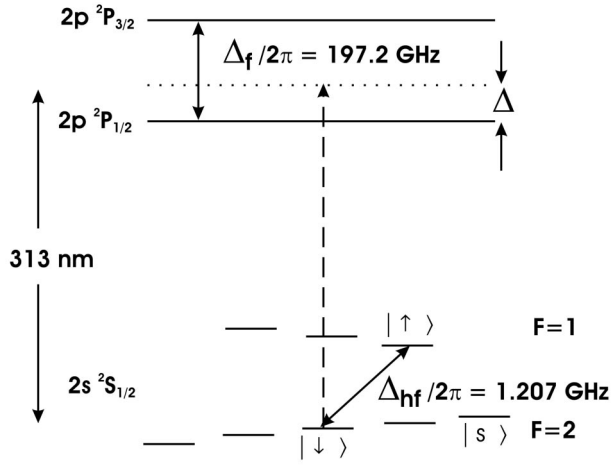

FIG. 1. The relevant energy levels of $^9Be^+$. The ground-state $2s\ ^2S_{1/2}$ manifold consists of the $F = 1$ and $F = 2$ hyperfine levels. Superposition states are composed of the $|F = 1, m_F = 1\rangle \equiv |\uparrow\rangle$ and $|F = 2, m_F = 0\rangle \equiv |\downarrow\rangle$ states. The excited-state $2p\ ^2P$ manifold consists of the $J = 1/2$ and $J = 3/2$ fine-structure levels, separated by $\Delta_f/2\pi = 197.2$ GHz. The laser frequency, illustrated by the dashed arrow, is detuned by Δ from the $|\downarrow\rangle$ to $^2P_{1/2}$ transition frequency.

$$\Gamma_{i,f} = g^2\gamma|\frac{a_{i\to f}^{(1/2)}}{\Delta} + \frac{a_{i\to f}^{(3/2)}}{\Delta - \Delta_f}|^2. \quad (1)$$

Here, $g = E\mu/2\hbar$, $E = \sqrt{2I/c\epsilon_0}$ is the laser-beam electric field amplitude, c is the speed of light, ϵ_0 is the vacuum dielectric constant, and $\mu = |\langle 2P_{3/2}, F = 3, m_F = 3|\boldsymbol{d}\cdot\hat{\sigma}_+|2S_{1/2}, F = 2, m_F = 2\rangle|$, where $\boldsymbol{d}$ is the electric-dipole operator. The effective amplitude $a_{i\to f}^{(J)} = \sum_q\sum_{e\in J}\langle f|\boldsymbol{d}\cdot\hat{\sigma}_q|e\rangle\langle e|\boldsymbol{d}\cdot\hat{\sigma}_k|i\rangle/\mu^2$ is the sum over amplitudes of scattering through all levels, $|e\rangle$, in the ^2P_J manifold, Δ is the laser detuning from the $^2S_{1/2} \to {}^2P_{1/2}$ transition, and $\gamma/2\pi = 19.4$ MHz is the radiative linewidth of the excited states in the ^2P manifold [16].

The Raman scattering rate, Γ_{Raman}, is given by summing over all the rates given by Eq. (1) where $i \neq f$. The Rayleigh scattering rate, Γ_{Rayleigh}, is that when $i = f$, and $\Gamma_{\text{total}} = \Gamma_{\text{Raman}} + \Gamma_{\text{Rayleigh}}$. The matrix elements $a_{i\to f}^{(1/2)}$ and $a_{i\to f}^{(3/2)}$ are identical in magnitude and opposite in sign for Raman scattering, whereas they are equal in sign for Rayleigh scattering. Therefore, when $|\Delta| \gg \Delta_f$ the two amplitudes in Eq. (1) destructively interfere to suppress Raman relative to Rayleigh scattering. In this limit the total scattering rate decreases as $1/\Delta^2$, whereas Raman scattering alone scales as $1/\Delta^4$. This suppression of population-changing Raman spontaneous scattering has been observed previously by Cline *et al.* [15].

In our experiment, a single trapped $^9Be^+$ ion in a superposition of two hyperfine states is illuminated by off-resonant laser light. The coherence and population relaxation rates are measured. The population relaxation rate provides the Raman photon scattering rate, which is then compared to the decoherence rate for different laser detunings.

We encode the superposition into the $|F = 1, m_F = 1\rangle \equiv |\uparrow\rangle$ and $|F = 2, m_F = 0\rangle \equiv |\downarrow\rangle$ ground states. At a magnetic field of 0.01194 T, the two levels are separated by $\Delta_{\text{hf}}/2\pi = 1.207$ GHz. At this field the energy difference between these two states does not depend to first order on changes in the magnetic field, and hence decoherence due to ambient magnetic field fluctuations is negligible [17].

The ion is confined in a linear Paul trap, and its motional and internal states are initialized by Doppler cooling and optical pumping into the $|^2S_{1/2}, F = 2, m_F = 2\rangle \equiv |s\rangle$, "stretched" state. Raman transitions between different hyperfine states are driven by a pair of copropagating Raman beams, detuned by $\Delta/2\pi \simeq 82$ GHz, and separated by the relevant hyperfine transition frequency. A resonant Raman pulse transfers the ion population from $|s\rangle$ to $|\uparrow\rangle$. Further Raman pulses are applied to manipulate the superposition between the $|\uparrow\rangle$ and $|\downarrow\rangle$ states. In a Bloch sphere representation [18], the rotation angle of a given pulse, θ, can be varied by changing the pulse duration. A π pulse is typically achieved with a duration of $\simeq 5$ μs. We measure the coherence of the state $\frac{1}{\sqrt{2}}(|\downarrow\rangle + |\uparrow\rangle)$ using the Ramsey method of separated fields [19]. This state is created with a $\pi/2$ pulse that is applied to $|\uparrow\rangle$. After a certain duration, a second $\pi/2$ pulse is applied with a phase ϕ_R relative to the first pulse, where ϕ_R can be varied. The population in the $|\uparrow\rangle$ state is then measured by transferring this population to the state $|s\rangle$ followed by state-dependent resonance fluorescence [5]. During a 200 μs detection pulse, we typically detect 12 photons if the ion is in the $|s\rangle$ state and approximately one photon if it is not.

To study decoherence, we illuminate the ion with a detuned, $\hat{\sigma}_+$ polarized beam that is inserted between the two Ramsey pulses. The decohering beam intensity has to be stabilized ($\lesssim 0.1\%$) to suppress Stark shift phase-noise decoherence. In addition, a spin-echo sequence is imple-

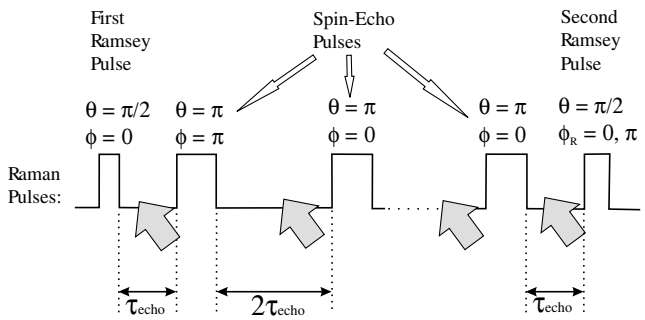

FIG. 2. Coherence relaxation pulse sequence. Two Ramsey pulses surround a sequence of spin-echo π pulses of alternating phase. The spin-echo pulses are separated by a time $2\tau_{\text{echo}}$, during which the ion is illuminated by a decohering beam, illustrated by the gray-filled arrows.

mented to limit the bandwidth of remaining phase noise to which the superposition is susceptible [18].

A typical experimental sequence is depicted in Fig. 2. After a duration τ_{echo} following the first Ramsey pulse, a sequence of π pulses, separated by $2\tau_{\text{echo}}$, is applied. The phase of subsequent π pulses alternates between 0 and π in order to correct for inaccuracies in the rotation angle. Between the spin-echo pulses the ion is illuminated by the decohering beam. The number of π pulses is determined by the maximum allowable value of τ_{echo} ($\simeq$10 ms) and varies for different decohering beam detunings between 2 and 18. At a duration τ_{echo} after the final π pulse, the final Ramsey pulse is applied. The experiment is run twice, once when ϕ_R, the phase of the final Ramsey pulse, equals 0, and once when it equals π. The population of the $|\uparrow\rangle$ state is subsequently measured. These two phases have been experimentally verified to provide the minimum and maximum signals for a range of ϕ_R, and therefore the signal difference corresponds to the Ramsey contrast and superposition coherence. The decrease of this difference as a function of the decohering beam duration, τ, is therefore a measure of the decoherence rate, independent of population relaxation.

The filled circles in Fig. 3 present the two measured Ramsey signals versus τ at a decohering beam detuning of $\Delta/2\pi = 227.5$ GHz. The upper filled circles correspond to the $\phi_R = \pi$ measurements, whereas lower filled circles are the $\phi_R = 0$ measurements. For $\tau \gtrsim 1$ ms, the two traces are seen to collapse on top of each other. The two curves do not collapse around their initial average value because population relaxation happens on the same time scale as decoherence. The decoherence time, τ_{dec}, is found by an exponential fit of the difference between the two curves.

The empty circles in Fig. 3 show the data from an identical experiment, except for the absence of the decohering beam. As can be seen, no significant decoherence can be measured during the measurement time in the absence of light.

We next measure the rates of population relaxation. The ion is prepared in either the $|\uparrow\rangle$ or the $|\downarrow\rangle$ state and illuminated by the decohering beam light for a variable time τ. The relevant state is then transferred to $|s\rangle$ before detection. The gray-filled squares in Fig. 3 show the decay in signal when the ion is prepared in the $|\uparrow\rangle$ state for $\Delta/2\pi = 227.5$ GHz. The decay of this signal is seen to agree with the decay in the Ramsey, $\phi_R = \pi$, signal. Very similar curves are measured when the ion is prepared in the $|\downarrow\rangle$ state.

For our initial conditions and laser polarization, the dynamics of population relaxation of both the $|\uparrow\rangle$ and $|\downarrow\rangle$ states can be modeled by the solution of two coupled rate equations with independent loss rates,

$$P(t) = \frac{1}{2\alpha} e^{-\beta t}[\kappa \sinh(\alpha t) + 2\alpha \cosh(\alpha t)]. \qquad (2)$$

The constants α, β, and κ are different for the $|\uparrow\rangle$ and $|\downarrow\rangle$

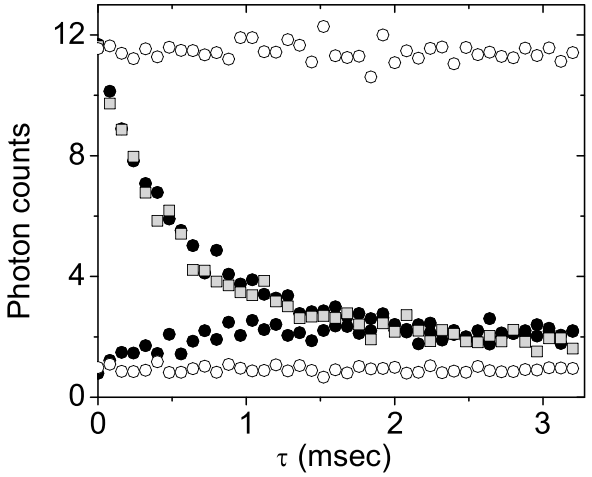

FIG. 3. Coherence and population relaxation data for a decohering beam detuning of $\Delta/2\pi \simeq 227.5$ GHz. The difference between the two filled circles curves is proportional to the superposition coherence at different times in the presence of the decohering beam light. The difference between the two open circles curves is proportional to the coherence in the absence of light. The gray-filled squares are proportional to the $|\uparrow\rangle$ state population at different times. Very similar data were recorded for the $|\downarrow\rangle$ state population. Every point in the figure is the average photon count of 400 experiments.

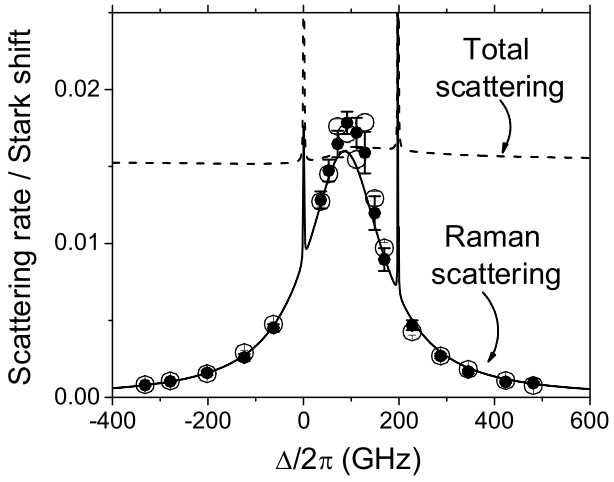

FIG. 4. Ratios of the different scattering rates and the decoherence rate to the differential Stark shift for different decohering beam detunings. The dashed line is the calculated $\Gamma_{\text{total}}/\Delta_{\text{St}}$, which at large detunings is seen to asymptotically reach a constant value of $\simeq 0.0154$. The solid line is the calculated $\Gamma_{\text{Raman}}/\Delta_{\text{St}}$. The empty circles are the measured values of $\Gamma_{\text{Raman}}/\Delta_{\text{St}}$ which are seen to be in reasonable agreement with the calculated curve. The filled circles are the measured values of $1/(\tau_{\text{dec}}\Delta_{\text{St}})$. The two sets of data are seen to be in good agreement, thus demonstrating that Raman scattering of photons is the dominant cause of decoherence. The suppression of the decoherence rate relative to the total scattering rate is evident for large detunings.

states, and, in both cases, can be related to Γ_{Raman}. We extract Γ_{Raman} by fitting curves such as shown by the gray-filled squares in Fig. 3 to Eq. (2).

We normalize the measured rates by the measured Stark shift, Δ_{St}, in the $|\downarrow\rangle \rightarrow |\uparrow\rangle$ transition frequency due to the decohering light, which serves as an independent measurement of the laser intensity on the ion. The Stark shift is measured by scanning the frequency of the Ramsey pulses and observing the shift of the Ramsey fringes with the decohering beam applied in between the pulses.

We calculate Δ_{St} by evaluating the difference in the Stark shift of the two levels,

$$\Delta_{\mathrm{St}} = g^2 \left(\frac{a^{(1/2)}_{|\uparrow\rangle\rightarrow|\uparrow\rangle}}{\Delta + \Delta_{\mathrm{hf}}} + \frac{a^{(3/2)}_{|\uparrow\rangle\rightarrow|\uparrow\rangle}}{\Delta + \Delta_{\mathrm{hf}} - \Delta_f} - \frac{a^{(1/2)}_{|\downarrow\rangle\rightarrow|\downarrow\rangle}}{\Delta} - \frac{a^{(3/2)}_{|\downarrow\rangle\rightarrow|\downarrow\rangle}}{\Delta - \Delta_f} \right). \tag{3}$$

The amplitudes $a^{J}_{|\uparrow\rangle\rightarrow|\uparrow\rangle}$ and $a^{J}_{|\downarrow\rangle\rightarrow|\downarrow\rangle}$ are almost equal and the difference in Stark shift is due primarily to the difference in detuning between the two hyperfine states. For $|\Delta| \gg \Delta_{\mathrm{hf}}$, the differential Stark shift decreases according to $1/\Delta^2$. The dashed line in Fig. 4 shows $\Gamma_{\mathrm{total}}/\Delta_{\mathrm{St}}$, the calculated total number of photons which are scattered for 1 rad of Stark phase evolution. This number asymptotically reaches a constant value of $0.9579\gamma/\Delta_{\mathrm{hf}} \simeq 0.0154$. As all of the measured data were taken in the $|\Delta| \gg \Delta_{\mathrm{hf}}$ limit the measured Δ_{St} is a good measure of the total scattering rate, almost independent of Δ. The solid line shows the calculated number of Raman scattered photons during the same cycle, $\Gamma_{\mathrm{Raman}}/\Delta_{\mathrm{St}}$. This number decreases as $1/\Delta^2$ for large laser detunings.

The empty circles in Fig. 4 present the measured $\Gamma_{\mathrm{Raman}}/\Delta_{\mathrm{St}}$ versus the decohering beam detuning. The measured data are seen to be in reasonable agreement with the theoretical prediction (solid line).

The filled circles in Fig. 4 show the measured ratio between the decoherence rate and the differential Stark shift, $1/(\tau_{\mathrm{dec}}\Delta_{\mathrm{St}})$, versus the detuning. As can be seen the measured points are in reasonable agreement with both the measured and the calculated $\Gamma_{\mathrm{Raman}}/\Delta_{\mathrm{St}}$ and are well below the $\Gamma_{\mathrm{total}}/\Delta_{\mathrm{St}}$ trace. For $\Delta/2\pi = -331.8$ GHz more than 19 photons are scattered on average before coherence is lost.

Spin-changing suppression when $|\Delta| \gg \Delta_f$ also causes the Rabi frequencies of stimulated Raman transitions to scale as $1/\Delta^2$. The total number of photons that are scattered during a 2π pulse asymptotically reaches a constant value proportional to $2\pi\gamma/\Delta_f$ [20]. However, since it is only Raman scattering that decoheres a hyperfine-state superposition, infidelities due to spontaneous scattering of photons will decrease as $1/\Delta^2$ for $|\Delta| \gg \Delta_f$.

In summary, we have measured the decoherence of superposition states of atomic hyperfine levels caused by spontaneous scattering of light. The data demonstrate that decoherence is dominated by Raman inelastic scattering. This rate can be quite small compared to the total scattering rate if the frequency of the light is detuned from the relevant excited level by more than its fine-structure splitting. The total scattering rate therefore gives a pessimistic measure of decoherence [20,21]. This has important implications for high-resolution spectroscopy and quantum-state manipulation.

We thank Chris Oates, John Bollinger, and Signe Seidelin for helpful comments on the manuscript. The work is supported by NSA/ARDA and NIST. Contribution of NIST; not subject to U.S. copyright.

*Present address: Department of Physics, University of IL at Urbana-Champaign, Urbana, IL 61801-3080.
†Present address: Department of Physics, Technion, Haifa 32000, Israel.

[1] A. Bauch and H. R. Telle, Rep. Prog. Phys. **65**, 789 (2002).
[2] H. J. Lewandowski, D. M. Harber, D. L. Whitaker, and E. A. Cornell, Phys. Rev. Lett. **88**, 070403 (2002).
[3] S. Gupta *et al.*, Science **300**, 1723 (2003).
[4] *Proceedings of the 18th International Conference of Atomic Physics (ICAP 2002)*, edited by H. R. Sadeghpour, E. J. Heller, and D. E. Pritchard (World Scientific, Singapore, 2003).
[5] D. J. Wineland *et al.*, J. Res. Natl. Inst. Stand. Technol. **103**, 259 (1998).
[6] M. F. Andersen, A. Kaplan, and N. Davidson, Phys. Rev. Lett. **90**, 023001 (2003).
[7] S. Kuhr *et al.*, Phys. Rev. Lett. **91**, 213002 (2003).
[8] M. B. Plenio and P. L. Knight, Phys. Rev. A **53**, 2986 (1996).
[9] C. Cohen-Tannoudji, Ann. Phys. (Paris) **7**, 423 (1962).
[10] B. B. Blinov, D. L. Moehring, L.-M. Duan, and C. Monroe, Nature (London) **428**, 153 (2004).
[11] C. Di Fidio and W. Vogel, Phys. Rev. A **62**, 031802 (2000).
[12] B. R. Mollow, Phys. Rev. **188**, 1969 (1969).
[13] J. T. Höffges, H. W. Baldauf, T. Eichler, S. R. Helmfrid, and H. Walther, Opt. Commun. **133**, 170 (1997).
[14] R. Loudon, *The Quantum Theory of Light* (Clarendon, Oxford, 1983).
[15] R. A. Cline, J. D. Miller, M. R. Matthews, and D. J. Heinzen, Opt. Lett. **19**, 207 (1994).
[16] In Eq. (1), we neglect the Zeeman and hyperfine splitting of the ground and excited states. The plots in Fig. 4, however, are the result of a calculation that takes these splittings into account.
[17] C. Langer *et al.*, quant-ph\0504076.
[18] L. Allen and J. H. Eberly, *Optical Resonance and Two-Level Atoms* (Dover, New York, 1975).
[19] N. Ramsey, Rev. Mod. Phys. **62**, 541 (1990).
[20] D. J. Wineland *et al.*, Phil. Trans. R. Soc. A **361**, 1349 (2003).
[21] Most multiqubit entangling gates for ions rely on the ions' motion being in the Lamb-Dicke regime. Ion heating due to photon scattering, although quadratically suppressed by the Lamb-Dicke parameter, can therefore degrade the fidelity of such gates.